

SUPPORTING INFORMATION FOR

h ν SABR: Photochemical Dose-Response Bead Screening in Droplets

*Alexander K. Price, Andrew B. MacConnell and Brian M. Paegel**

Department of Chemistry, The Scripps Research Institute, Jupiter, FL 33458, United States

SUPPORTING INFORMATION EXPERIMENTAL SECTION

PC-FAM solid-phase synthesis and characterization. Synthesis resin (TentaGel M NH₂, 10 μ m dia., 10 mg, 0.23 mmol/g and and Tentagel RAM, 160 μ m dia., 1.5 mg, 0.43 mmol/g, Rapp Polymere GmbH, Tuebingen, Germany) were loaded into a spin column (Mobicol, 10- μ m pore, Boca Scientific, Boca Raton, FL) and swelled in DMF (1 h, RT). Fmoc-Gly-OH (20 μ mol), COMU (20 μ mol) and DIEA (40 μ mol) were combined in DMF (0.4 mL), added to the resin and reacted (15 min, RT). The coupling cycle was repeated once and the resin washed with DMF (3 x 0.6 mL). Carboxylic acid monomer coupling for all subsequent solid-phase synthesis followed this protocol. The Fmoc-protected resin was deprotected in piperidine (20% v/v in DMF, 2 x 0.5 mL, 10 min each aliquot, RT) and washed (DMF, 3 x 0.6 mL; DCM, 3 x 0.6 mL; DMF, 3 x 0.6 mL). Fmoc deprotection and washing for all subsequent solid-phase synthesis followed this protocol. Fmoc-photolabile linker (32 μ mol), DIC (50 μ mol), 2,4,6-trimethylpyridine (TMP, 32 μ mol) and ethyl (hydroxyimino)cynoacetate (Oxyma, 32 μ mol) were combined in DMF (0.4 mL), added to the resin and reacted (3 h, 37 °C, x2) and the resin washed (DMF, 3 x 0.6 mL). Unreacted amines were acetylated (20% v/v acetic anhydride in DMF, 20 min, RT) prior to Fmoc deprotection and further cycles of monomer coupling (20 μ mol acid, 20 μ mol COMU, 40 μ mol DIEA). The resin was functionalized with the following monomer sequence: Fmoc-(PEG)₂-CH₂CH₂COOH, Fmoc-Glu(OtBu)-OH, and Fmoc-(PEG)₂-CH₂CH₂COOH. The N terminus was fluorescently labeled by adding a solution of 5(6)-carboxyfluorescein (20 μ mol) and DIEA (40 μ mol) activated with COMU (20 μ mol) to the resin in DMF (0.4 mL), reacting (30 min, RT, x2), and washing (DMF, 3 x 0.6 mL). The 10- μ m resin was separated from the 160- μ m resin via filtration (Partec CellTrics 150 μ m, Sysmex America, Lincolnshire, IL) and the t-butyl protecting group on the glutamic acid was removed with trifluoroacetic acid (TFA, 95%

v/v in DCM, 0.4 mL, 1 h, RT, x2). The resin was washed (DMF, 6 x 0.6 mL) and stored protected from light in DMF (-20 °C). A 0.5-mg aliquot of 160- μ m resin was simultaneously deprotected and cleaved (TFA/DCM/triisopropylsilane (TIPS), 90:5:5, 1 h, RT). The supernatant was collected, dried down and resuspended (50% v/v ACN in 0.1% TFA in water). G-PC-PEG₂-E-PEG₂-FAM solution (1 μ L) was spotted on a MALDI target plate, dried, covered with HCCA matrix solution (10 mg/mL in 50% v/v ACN/0.1% TFA in water), and subjected for MALDI-TOF analysis (Figure S3) in negative ionization mode (Microflex LT, Bruker, Billerica, MA).

PC-Pepstatin A solid-phase synthesis and characterization. TentaGel M NH₂ synthesis resin (10 μ m dia., 15 mg, 0.25 mmol/g, Rapp Polymere GmbH) was mixed with Tentagel RAM resin (160 μ m dia., 1.5 mg, 0.43 mmol/g, Rapp Polymere GmbH), loaded into a spin column (Mobicol, 10 μ m pore, Boca Scientific), swelled and deprotected (20% v/v piperidine in DMF, 1 h, RT). The resin was washed (DMF, 3 x 0.6 mL; DCM, 3 x 0.6 mL; DMF, 3 x 0.6 mL). Fmoc-Gly-OH (40 μ mol), COMU (40 μ mol), and DIEA (80 μ mol) were combined in DMF, added to the resin, and reacted (15 min, RT). This coupling protocol was repeated once and the resin was washed (DMF, 3 x 0.6 mL). Carboxylic acid coupling for all subsequent solid-phase synthesis followed this protocol. The Fmoc-protected resin was deprotected (20% v/v piperidine, 10 min, RT, x2) and washed (DMF, 3 x 0.6 mL; DCM, 3 x 0.6 mL; DMF, 3 x 0.6 mL). Fmoc deprotection and washing for all subsequent solid-phase synthesis followed this protocol. Fmoc-photolabile linker (60 μ mol), DIC (120 μ mol), TMP (60 μ mol), and Oxyma (60 μ mol) were combined in DMF (0.4 mL), added to the resin, and reacted (2 h, 37 °C), and the resin washed (DMF, 3 x 0.6 mL). Unreacted amines were acetylated (20% v/v acetic anhydride in DMF, 20 min, RT) prior to Fmoc deprotection and further functionalization with Fmoc-Glu(OtBu)-OH (40 μ mol acid, 40 μ mol COMU, and 80 μ mol DIEA in 0.4 mL DMF). Pepstatin A was conjugated to

the N-terminus by preparing a solution of pepstatin A (8 μ mol), DIC (64 μ mol), TMP (16 μ mol), and Oxyma (16 μ mol) in DMF (0.4 mL), adding to the resin, and reacting (1 h, 70 °C). The 10- μ m resin was separated from the 160- μ m resin via filtration (Partec CellTrics 150 μ m, Sysmex America) and the t-butyl protecting group on the glutamic acid was removed with TFA (95% v/v in DCM, 0.5 mL, 1 h, RT, x2). The resin was washed (DMF, 6 x 0.6 mL) and stored protected from light in DMF (-20 °C). The PC-E-pepstatin A-resin (160- μ m RAM resin, 0.5 mg) was simultaneously deprotected and cleaved (TFA/DCM/TIPS, 90:5:5, 1 h, RT). The supernatant was collected, dried down and resuspended (20% v/v in 0.1% TFA in water). G-PC-E-pepstatin A solution (1 μ L) was spotted on a MALDI target plate and mass analyzed as above (Figure S5).

Confocal laser-induced fluorescence detection system. Droplet fluorescence was detected on-chip using a two-channel confocal laser-induced fluorescence (LIF) microscope that was built in-house using 30-mm cage system components (Thorlabs, Inc., Newton, NJ). A long-pass dichroic mirror (505 DRLP, Omega Optical Inc., Brattleboro, VT) directs light from a 488-nm laser (OBIS-488 20LS, Coherent Inc., Santa Clara, CA) into a microscope objective (40X, 0.60 NA, 2.8 mm WD, Motic, Richmond, Canada), which focuses the excitation beam on the microfluidic channel and collects fluorescence emission. The dichroic transmits the emission signal to a shortpass dichroic (550 DRSP, Edmund Optics, Barrington, NJ). Emitted light between 505 and 550 nm is spectrally filtered through a bandpass filter (520DF10, Omega Optical) before being focused by a plano-convex lens ($f/D = 30$ mm/25.4 mm). A pinhole (100 μ m) spatially filters the focused light prior to detection with a photon counting head PMT (H7828, Hamamatsu, Middlesex, NJ). Emitted light longer than 550 nm is directed to a longpass dichroic (600 DRLP, Edmund Optics), which reflects light between 550 and 600 nm to a bandpass filter (570DF10, Omega Optical) and an otherwise identical plano-convex

lens/pinhole/PMT optical train. The PMT signals are digitized by a data acquisition board (NI-USB-6341, National Instruments, Austin, TX). LabVIEW code written in-house controls acquisition. An illumination system (Schott ACE, Schott AG, Mainz, Germany) equipped with a gooseneck fiber and 610-nm cut-on glass filter (Newport Corporation, Irvine, CA) is used to image the microfluidic device with a high-speed camera (NR4S1, Integrated Design Tools, Tallahassee, FL). For waveguide calibration experiments, a neutral density filter (3.0 OD, ThorLabs) was installed at the front end of the detection system to attenuate laser power.

Calibration of UV waveguide exposure. Droplets encapsulating PC-FAM beads (Figure S3) were dispensed into wells. Droplets were dosed with UV light from a X-Cite 120Q lamp (Lumen Dynamics Group Inc., Mississauga, Canada) through an open objective port on an inverted epifluorescence microscope using Zeiss filter set 49 ($\lambda_{\text{ex}} = 365 \text{ nm}$; $\lambda_{\text{dc}} = 395 \text{ nm}$; $\lambda_{\text{em}} = 445/50 \text{ nm}$). Exposure energy ($0.5\text{-}304 \text{ J/cm}^2$) was measured using a photometer equipped with an I-line sensor (ILT 1400-A & XRL340B, International Light Technologies, Peabody, MA). Droplets were imaged (10X, 0.25 NA) in both bright field and fluorescence mode through Zeiss filter set 38HE ($\lambda_{\text{ex}} = 470/40 \text{ nm}$; $\lambda_{\text{dc}} = 495 \text{ nm}$; $\lambda_{\text{em}} = 525/50 \text{ nm}$). Image data were analyzed (ImageJ) to determine droplet size, bead size, and mean droplet fluorescence. Image data featuring droplets of 3, 10, 30 and 100 μM fluorescein were analyzed in the same way to generate a calibration curve ($r^2 = 0.99$), which was used to assign fluorescein concentration to UV exposures (Figure S6). Likewise, UV exposures were assigned to the waveguide by correlating the BV570 emission intensity generated during waveguide calibration to the fluorescence generated in the droplet using the fitting curves of Figures 3D and S6.

Figure S1

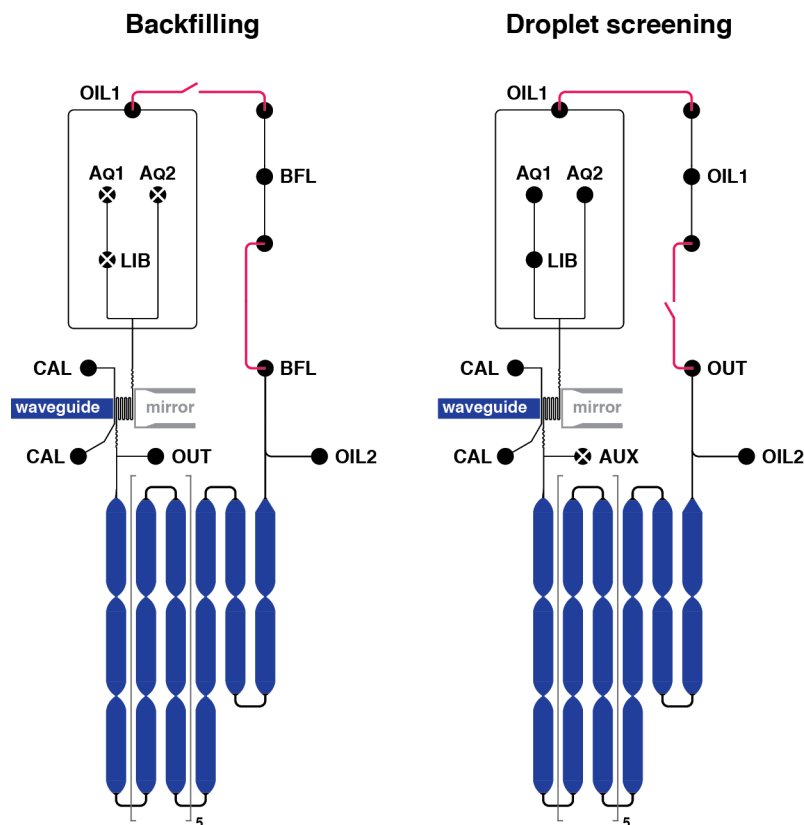


Figure S1. Operational modes for the integrated droplet-based assay circuit. Prior to droplet screening mode, the incubation channel is backfilled with oil phase from the BFL and OIL2 inputs. The microbore Tygon tubing connector (magenta) between the BFL input and the OIL1 reservoir is clamped. As oil approaches the output (OUT) near the illumination region, aqueous phase is pumped into the AQ1 and AQ2 inputs, and the connector between BFL and OIL1 is unclamped, splitting the oil flow between backfilling and droplet formation. To initiate droplet screening, the connector between OIL1 and OUT is clamped and a waste tube is inserted into the output reservoir, forcing the oil flow to OIL1 for droplet formation. Finally, the waste tubing in the AUX/OUT output is clamped, diverting droplet flow into the incubation channel.

Figure S2

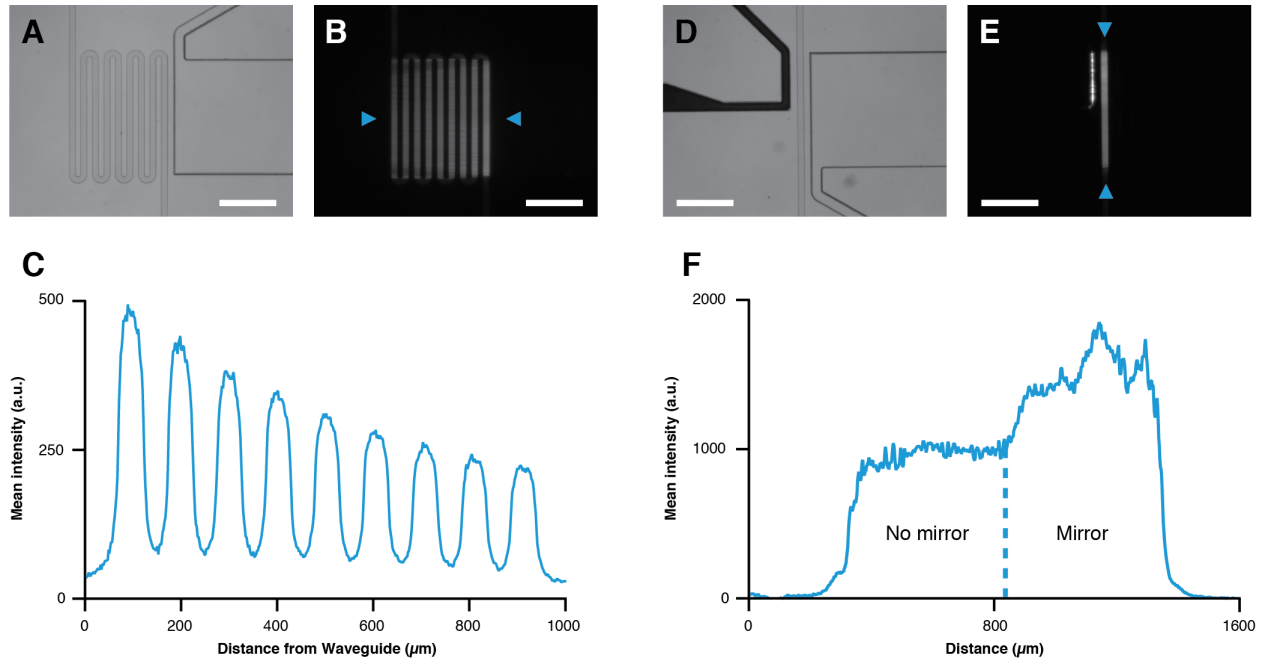


Figure S2. Serpentine and microsolidic mirror illumination region components. Brightfield (A) and fluorescence (B) micrographs showing a nine-pass serpentine channel adjacent a microfabricated optical waveguide (scale = 500 μm). (C) A line scan taken through the center of the illumination region (panel B, between the blue markers) shows a decrease in the fluorescence emission of cascade blue-conjugated dextran as distance from the waveguide increases. Brightfield (D) and fluorescence (E) micrographs showing a microsolidic mirror used to enhance UV irradiation in the illumination region (scale = 500 μm). (F) A line scan taken through the center of the fluidic channel (panel E, between the blue markers) shows an increase in cascade blue fluorescence emission in the channel region between the waveguide and mirror compared to the region lacking a bounding mirror.

Figure S3

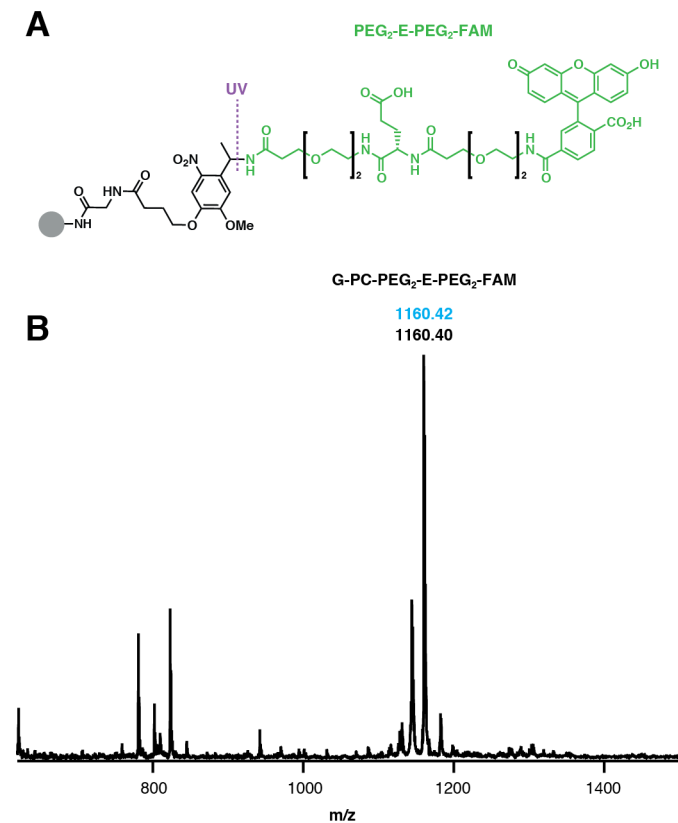


Figure S3. Photocleavable PEG₂-E-PEG₂-FAM. (A) The structure of the model compound on resin (gray circle) used in waveguide calibration experiments includes the PEG₂-E-PEG₂-FAM (green) fluorescent product of UV-induced *o*-nitrobenzyl linker photolysis. The ionizable carboxylic acid on the glutamate residue ensures that the model compound is retained in droplets after linker photolysis. A similar strategy using sulfonic acid groups has been implemented for droplet-based studies.¹ (B) Compound synthesized on TentaGel RAM resin was cleaved from the resin in acid to yield the full G-PC-PEG₂-E-PEG₂-FAM product. MALDI-TOF MS analysis of the cleavage product yielded a predominant [M+H]⁺ (black) in agreement with the theoretical exact mass (cyan).

Figure S4

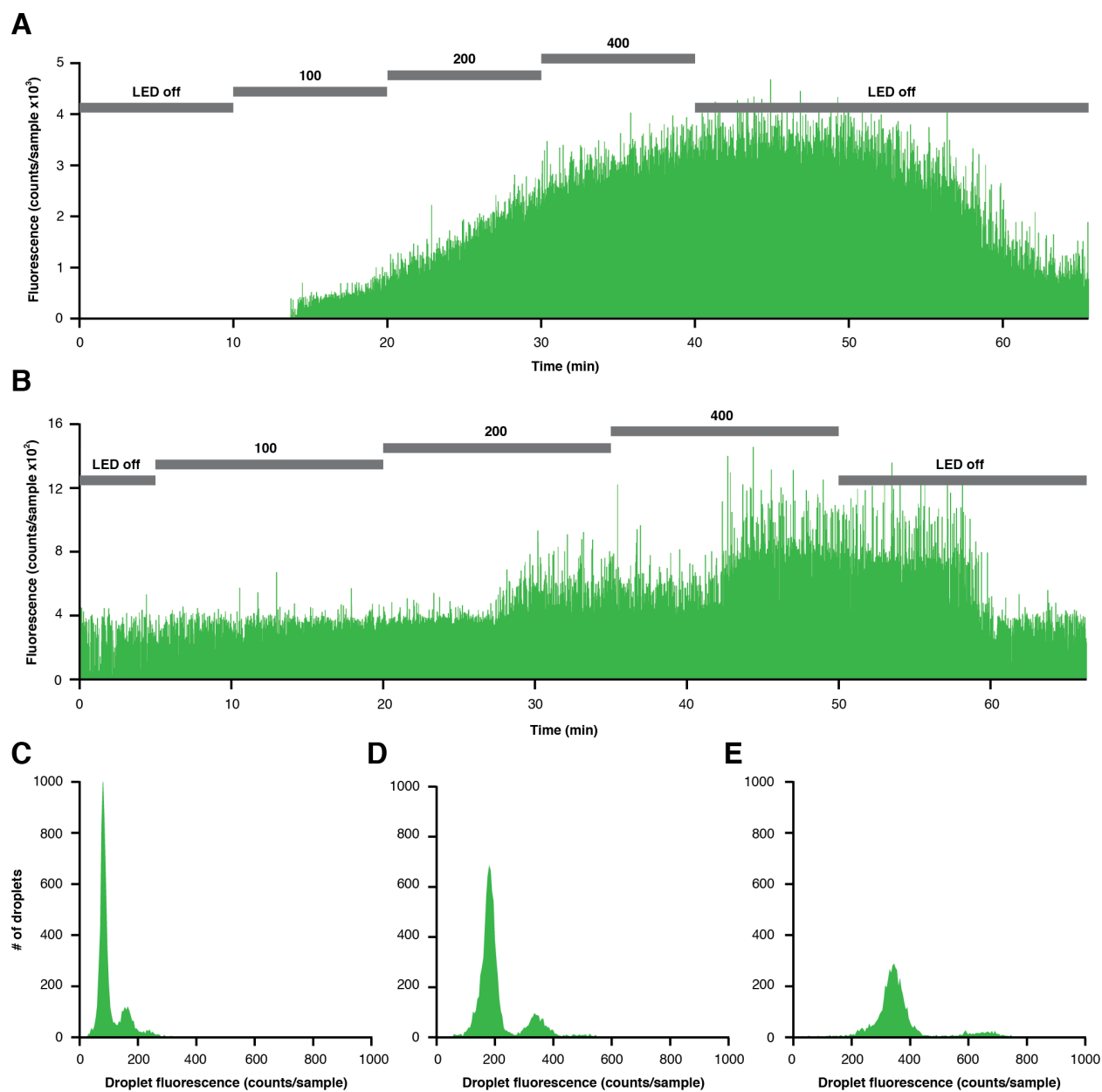


Figure S4. On-line photochemical dosing. Example data derived from a dosing experiment on devices (A) lacking or (B) including patterned avobenzene-doped PDMS. Without patterned avobenzene modification, droplets are continuously exposed to stray UV light as they navigate the incubation channel. The total droplet population exhibits a fluorescence profile that suggests

a smooth and continuous increase in UV intensity over the course of the experiment. The device with avobenzene-doped PDMS exhibits “step” transitions between UV intensities, in agreement with the abrupt user-programmed changes in UV intensity and supporting the conclusion that photolysis is restricted to the illumination region. Gray bars indicate the duration of a particular UV intensity (LED current shown in mA). Of note, the events that produce ~400 counts/sample across the entire run in (B) are spikes from fluorescent PC-FAM beads that pass through the detection volume; these spikes do not accurately represent the droplet fluorescence and are eliminated during data analysis. Histograms of selected data from the experiment in panel B each show the fluorescence profile for populations of > 4,000 occupied droplets that experience UV exposure correlating with LED currents of (C) 100 mA, (D) 200 mA, and (E) 400 mA.

Figure S5

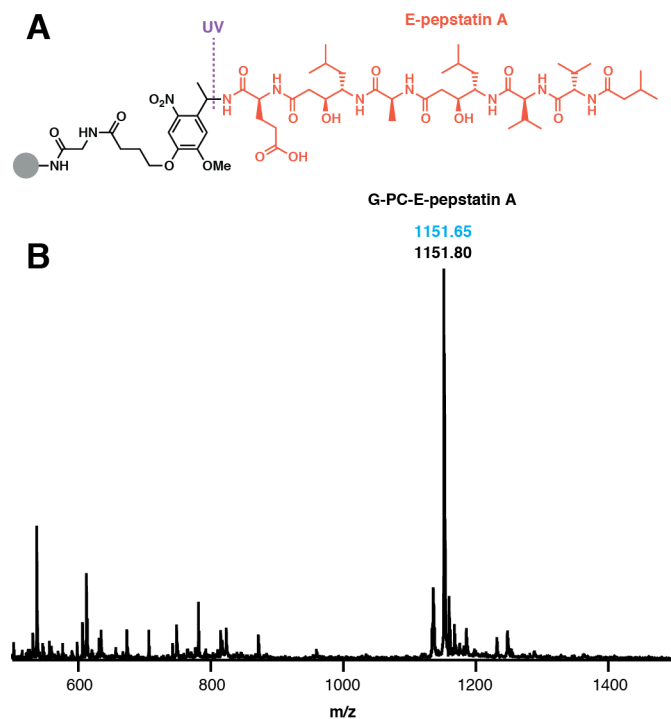


Figure S5. Photocleavable E-pepstatin A. (A) The structure of the positive control inhibitor on resin (gray circle) used in the HIV-1 protease biochemical activity assay includes the E-pepstatin A (red) inhibitor product of UV-induced *o*-nitrobenzyl linker photolysis. The glutamate residue installed on the C-terminus of pepstatin A restores a carboxylic acid to the peptide and aids in molecular retention. (B) Compound synthesized on TentaGel RAM resin was cleaved from the resin in acid to yield the full G-PC-E-pepstatin A product. MALDI-TOF MS analysis of the cleavage product yielded a predominant $[M+H]^+$ (black) in agreement with the theoretical exact mass (cyan).

Figure S6

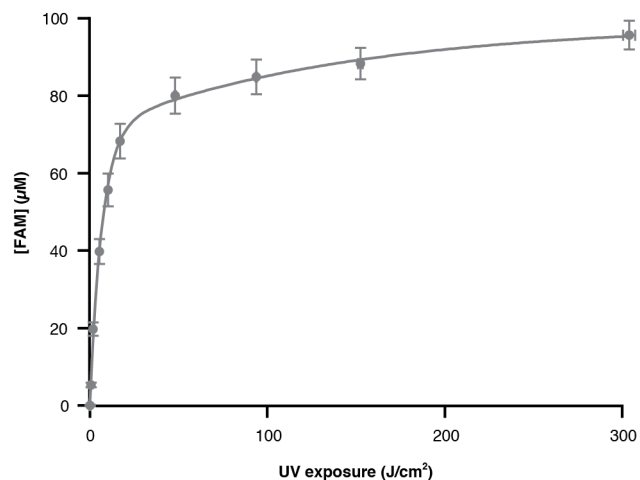


Figure S6. Photochemical dosing of droplets with PEG₂-E-PEG₂-FAM for determination of waveguide performance. Photolytic cleavage of PEG₂-E-PEG₂-FAM from the bead surface as a function of UV dose (n = 13 droplets, normalized volume = 200 pL) exhibits biphasic kinetics, which is common for *o*-nitrobenzyl photochemistry.^{2,4} The compound concentration plateaus above 90 μM at high UV doses.

Figure S7

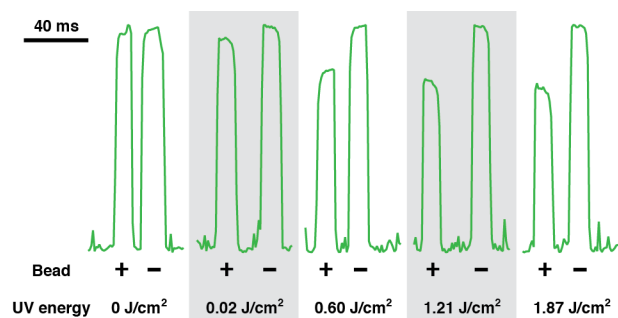


Figure S7. Example dose-response data for HIV-1 protease activity assay. Paired occupied (+) and empty (-) droplets demonstrate UV dose-dependent inhibition of HIV-1 protease activity with beads displaying E-pepstatin A. In the absence of compound cleavage, occupied droplets are indistinguishable from empty droplets. As UV dose increases, so does the concentration of E-pepstatin A, which results in inhibited proteolysis of the fluorogenic probe.

SUPPORTING INFORMATION REFERENCES

- (1) Woronoff, G.; El-Harrak, A.; Mayot, E.; Schicke, O.; Miller, O. J.; Soumillion, P.; Griffiths, A. D.; Ryckelynck, M. *Anal. Chem.* **2011**, *83*, 2852–2857.
- (2) Piggott, A. M.; Karuso, P. *Tetrahedron Lett.* **2005**, *46*, 8241–8244.
- (3) Kretschy, N.; Holik, A.-K.; Somoza, V.; Stengele, K.-P.; Somoza, M. M. *Angew. Chem. Int. Ed.* **2015**, *54*, 8555–8559.
- (4) Zhu, Q. Q.; Schnabel, W.; Schupp, H. *J. Photochem.* **1987**, *39*, 317–332.